

## RAPID COMMUNICATION

# Void fraction measurement in two-phase flow processes via symbolic dynamic filtering of ultrasonic signals

Subhadeep Chakraborty, Eric Keller, Justin Talley, Abhishek Srivastav, Asok Ray and Seungjin Kim

Department of Mechanical and Nuclear Engineering, The Pennsylvania State University, University Park, PA 16802, USA

Received 26 November 2008, in final form 18 December 2008

Published 20 January 2009

Online at [stacks.iop.org/MST/20/023001](http://stacks.iop.org/MST/20/023001)

## Abstract

This communication introduces a non-intrusive method for void fraction measurement and identification of two-phase flow regimes, based on ultrasonic sensing. The underlying algorithm is built upon the recently reported theory of a statistical pattern recognition method called symbolic dynamic filtering (SDF). The results of experimental validation, generated on a laboratory test apparatus, show a one-to-one correspondence between the flow measure derived from SDF and the void fraction measured by a conductivity probe. A sharp change in the slope of flow measure is found to be in agreement with a transition from fully bubbly flow to cap-bubbly flow.

**Keywords:** symbolic dynamics, parameter estimation, void fraction, two-phase flow, regime identification

(Some figures in this article are in colour only in the electronic version)

## 1. Introduction

In many two-phase flow systems, information on the void fraction plays a critical role in terms of system design and operation. For example, in nuclear reactors, knowledge of the void fraction is important since the plant dynamics may significantly change with increasing void fraction. In addition to affecting the heat transfer characteristics and coolant pressure drop of the reactor, it can influence the neutron flux distribution and destabilize the reactor power distribution.

Different techniques have been developed to measure void fraction in two-phase flow systems. Examples are side-tube methods [1], image analysis methods [2], densitometry methods [3, 4], impedance methods [5, 6], conductivity probe methods [7, 8] and ultrasonic methods [9, 10]. Even though each of these methods has its own advantages and disadvantages, computed tomography (CT) methods for two-phase flow measurements have gained in prominence due to significant advancements of this field in recent years. For

example, Bieberle *et al* [11] have investigated electron-beam CT arrangements for reconstructing cross-sectional images of two-phase flows, and Schleicher *et al* [12] have introduced the design of an optical tomograph. These methods are attractive as they enable recovery of the complete in-plane two-phase flow structure. However, they have limited practical applicability because of the need for a large array of sensors and associated instrumentation. In contrast, the electrical impedance method does not need such an arrangement. Along this line, Zhou *et al* [13] have developed a reconstruction technique that recovers instantaneous phase information of two-phase flow; however, this technique is invasive.

Ultrasonic methods offer an alternative option that has many benefits compared to other available methods. In addition to its non-invasive nature, the measurement system is portable, independent, and can be applied at many locations. However, the current ultrasonic methods are limited by the fact that they also rely on prior signal attenuation calibration, or tomography techniques that require an array of sensors.

This communication presents initial results of theoretical and experimental research toward demonstration of the feasibility of a single ultrasonic sensor to measure void fraction in (two-phase) air–water flow that includes a transition from fully bubbly flow to cap-bubbly flow.

A data-driven statistical time series analysis technique called symbolic dynamic filtering (SDF) [14] has been adopted in conjunction with *analytic signal space partitioning* (ASSP) [15] that is based on Hilbert transform preprocessing.

## 2. Review of underlying concepts

While the theories of analytic signal space partitioning (ASSP) and symbolic dynamic filtering (SDF) are reported in previous publications [14, 15], this section briefly presents their underlying principles for completeness of this communication.

### 2.1. Analytic signal-space partitioning

Analytic signal-space partitioning (ASSP) of time series data, which is based on Hilbert transform preprocessing, is used for symbol sequence generation that is an essential ingredient of symbolic dynamic filtering (SDF). Hilbert transform [16] of a real-valued signal  $x(t)$  is defined as

$$\tilde{x}(t) = \mathcal{H}[x](t) = \frac{1}{\pi} \int_{\mathbb{R}} \frac{x(\tau)}{t - \tau} d\tau. \quad (1)$$

That is,  $\tilde{x}(t)$  is the convolution of  $x(t)$  with  $\frac{1}{\pi t}$  over the real field  $\mathbb{R}$ , which is represented in the Fourier domain as

$$\mathcal{F}[\tilde{x}](\xi) = -i \operatorname{sgn}(\xi) \mathcal{F}[x](\xi), \quad (2)$$

where

$$\operatorname{sgn}(\xi) = \begin{cases} +1 & \text{if } \xi > 0 \\ -1 & \text{if } \xi < 0. \end{cases}$$

The corresponding complex-valued analytic signal [16] is defined as

$$\mathcal{A}[x](t) = x(t) + i\tilde{x}(t) \quad (3)$$

$$\mathcal{A}[x](t) = a(t) \exp(i\varphi(t)), \quad (4)$$

where  $a(t)$  and  $\varphi(t)$  are called the instantaneous amplitude and instantaneous phase of  $\mathcal{A}[x](t)$ , respectively.

The analytic signal generates a pseudo-phase plot by mapping the complex domain  $\mathbb{C}$  onto the two-dimensional real space  $\mathbb{R}^2$ , i.e., by assigning the real and imaginary parts of the analytic signal on  $x$  and  $y$  axes, respectively, in Cartesian coordinates, or the magnitude and angle of the analytic signal on  $r$  and  $\theta$  axes, respectively, in polar coordinates. In this setting, the time-dependent analytic signal in equation (3) is now represented as a (one-dimensional) trajectory in the two-dimensional pseudo-phase space.

**Remark 2.1.** It has been argued by Lee *et al* [17] that a seven-dimensional phase space representing different sets of data, such as void fraction, pressure, liquid velocity, vapor velocity, liquid temperature, vapor temperature and the interfacial area concentration, needs to be constructed as a first step in the analysis of the two-phase dynamical system. The (two-dimensional) pseudo-phase space is an alternative to the

multi-dimensional phase space that is usually constructed by embedding [18] of available sensor data.

Let  $\Xi$  be a compact region in the pseudo-phase space, which encloses the trajectory. The objective here is to partition  $\Xi$  into finitely many mutually exclusive and exhaustive segments, where each segment is labeled with a symbol and the resulting set of (finitely many) symbols is called the alphabet  $\Sigma$ . The segments are determined by magnitude and phase of the analytic signal and also from the density of data points in these segments. That is, if the magnitude and phase of a data point of the analytic signal lies within a segment or on its boundary, then that data point is labeled by the corresponding symbol. This process of symbol generation is called analytic signal space partitioning (ASSP) [15].

One possible way of partitioning  $\Xi$  is to divide the magnitude and phase of the time-dependent analytic signal in equation (3) into uniformly spaced segments between their minimum and maximum values. This is called uniform partitioning. An alternative method, known as maximum entropy partitioning [15], maximizes the entropy of the partition, which imposes a uniform probability distribution on the symbols. In this partitioning, parts of the state space with rich information are partitioned into finer segments than those with sparse information. The ASSP algorithm makes use of either one or both of these partitioning methods [15].

### 2.2. Symbolic dynamic filtering

Given a representative symbol sequence derived from the real-valued time series, the concept of  $D$ -Markov machine [14] has been adopted for the void fraction measurement system. The  $D$ -Markov machine has a state-space structure where the states of the machine are represented by blocks of symbols  $\sigma_i \sigma_{i+1} \sigma_{i+2} \dots \sigma_{i+D-1}$  in the symbol sequence. Thus, with cardinality  $|\Sigma|$  of the alphabet and depth  $D$  of a symbol string of a state, the total maximum number of states in the  $D$ -Markov machine is given by  $|\Sigma|^D$ . Thus, the state machine moves from one state to another upon occurrence of a symbol. All symbol sequences that have the same last  $D$  symbols represent the same state.

A change in the void fraction may cause deviation of the probability distribution of the states. A measure of this deviation, which is called the flow measure, is the distance between the state probability vectors at the nominal and off-nominal conditions. In this communication, the flow measure at the  $k$ th epoch is defined as

$$\mu_k = \arccos \left( \frac{\langle p_0, p_k \rangle}{\|p_0\|_2 \|p_k\|_2} \right), \quad (5)$$

where  $\langle p_0, p_k \rangle$  is the inner product of probability vectors  $p_0$  and  $p_k$  at the nominal condition and the  $k$ th epoch, respectively; and  $\|\bullet\|_2$  is the Euclidian norm of  $\bullet$ .

## 3. Experimental validation on a test apparatus

Figure 1 shows the schematic diagram of a test apparatus that has been custom built to experimentally validate the proposed concept of void fraction measurement by ultrasonic sensing.

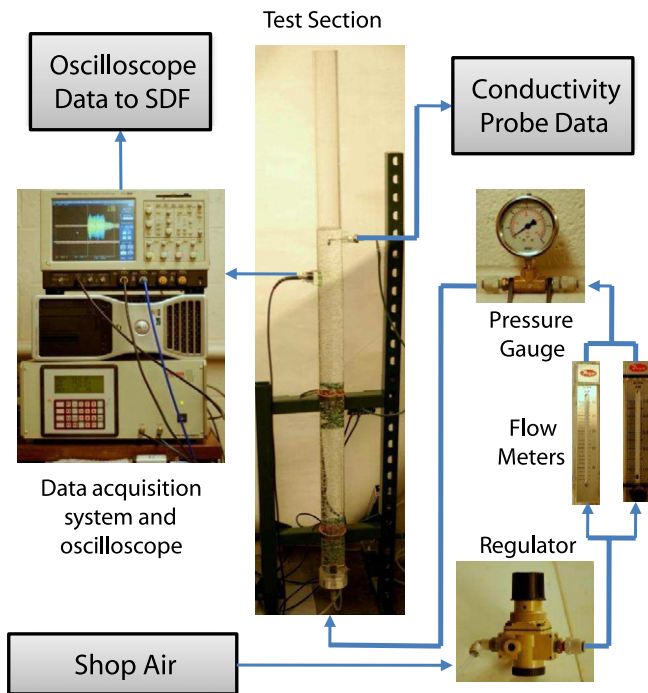


Figure 1. Schematic diagram of the experimental apparatus.

The vertical test section of the test apparatus is made of clear acrylic pipe with 50 mm inner diameter and 6.5 mm wall thickness; the total height of the apparatus is approximately 1.5 m. Compressed air is injected into the pipe through a sparger (with 10  $\mu\text{m}$  pores) that is located at the bottom, and the gas flow rate is measured by a gas rotameter. The gas flow rate, equivalent to the value under the atmospheric pressure condition, is calculated based on the back pressure measured by the local pressure gauge at the exit of the gas rotameter. The pressure regulator installed before the flow meter is used to control the gas flow rate.

### 3.1. Conductivity probe

To calibrate the ultrasonic sensor, the local time-averaged void fraction is measured by a single-sensor conductivity probe [8], located at  $\sim 1$  m (i.e.,  $z/D \approx 20$ ) above the bottom of the pipe. The radial position of the needle probe is manually adjustable by a traversing mechanism at any cross-section of the vertical pipe. In the experiments reported in this paper, the profiles of time-averaged two-phase flow parameters are measured by performing measurements at different radial locations. The local void fractions are measured by traversing the probe in the radial direction, the first being at 2 mm and the subsequent ones being at 4, 6, 8, 11, 14, 17, 20 and 25 mm away from the inner wall.

The sampling frequency of the needle probe measurements is chosen to be 6 kHz and the signal is recorded at each radial position for 60 s. The void fraction is measured at up to nine radial positions for each experiment with a net measurement time of 9 min for each flow condition. The conductivity probe measurement is based on the fundamental difference in the conductivity of water and air; each time a gas

bubble passes through the tip of the conductivity probe, the impedance of the connected electrical circuit changes. This time series signal is processed to yield the void fraction. For each probe position [8], the time-averaged local void fraction is obtained as the ratio of the sum of the residence time of individual bubbles and the total measurement time:

$$\alpha_i = \frac{\sum_j \Delta t_i^j}{T_i} \in [0, 1] \text{ at radius } r_i, \quad i = 1, \dots, N, \quad (6)$$

where  $\Delta t_i^j$  is the residence time of the  $j$ th bubble,  $T_i$  is the total measurement time at radius  $r_i$ , and  $N$  is the total number of time-averaged measurements. (Note:  $N = 9$  in this test setting.) For each flow rate condition, the total measurement time is adjusted to obtain enough bubble signals for reliable statistics of the time-averaged value. The spatial average  $\alpha$  of void fraction is numerically obtained based on the data set  $\{(r_i, \alpha_i), i = 1, \dots, N\}$  over the entire flow cross-sectional area.

### 3.2. Ultrasonic probe

In the test apparatus, the ultrasonic transducer is placed at a level of 0.86 m above the bottom of the pipe. To ensure uniformity of measurements, direction of the ultrasonic wave travel is aligned with the radial movement of the void fraction conductivity probe. A Matec PR5000 sine wave pulser/receiver is used to inject a pulsed sine wave ultrasonic wave into the pipe, as seen in figure 1. The signal is captured at the rate of 100 Mega samples per second by a National Instruments PCI-5122 oscilloscope card installed on a desktop computer. The oscilloscope is triggered using the digital trigger pulse generated by the pulser/receiver. An ultrasonic transducer (3.5 MHz 12.5 mm diameter Panametrics A415S) is placed on an acrylic block of thickness  $\sim 13.5$  mm that conforms to the outside diameter of the acrylic pipe; this makes a total thickness of  $\sim 20$  mm when added to the pipe wall of 6.5 mm thickness. The pulser/receiver is used in pulse-echo mode to produce a 3.5 MHz pulsed sine wave of 4.96  $\mu\text{s}$  duration at a repetition rate of 400 pulses per second. Only a portion of the resulting signal is used for analysis. Specifically, the first 600 samples correspond to the first echo returned upon reflection from the back wall on the inner surface of the pipe; this signal is measured with a delay of  $\sim 82 \mu\text{s}$ , which is the sum of  $\sim 67 \mu\text{s}$  delay due to the wave traveling a distance of 100 mm (i.e., twice the pipe's internal diameter) at the speed of sound  $c = 1500 \text{ m s}^{-1}$  in water, and  $\sim 15 \mu\text{s}$  delay due to the wave traveling a distance  $\sim 40$  mm (i.e., twice the total thickness of the traversed acrylic medium) at the speed of sound  $c = 2730 \text{ m s}^{-1}$ .

Reflections of individual ultrasonic pulses contain information corresponding to a time-localized snap-shot of the two-phase flow. However, relevant statistical information, which is representative of time-averaged flow condition, can only be extracted by compiling a large ensemble of pulses. Working with such a data set ensures that the effects of spatial distribution of voids are incorporated in the analysis. In these experiments, a data set of more than 1600 ultrasonic pulses, corresponding to  $\sim 4$  seconds, was used for each flow condition.

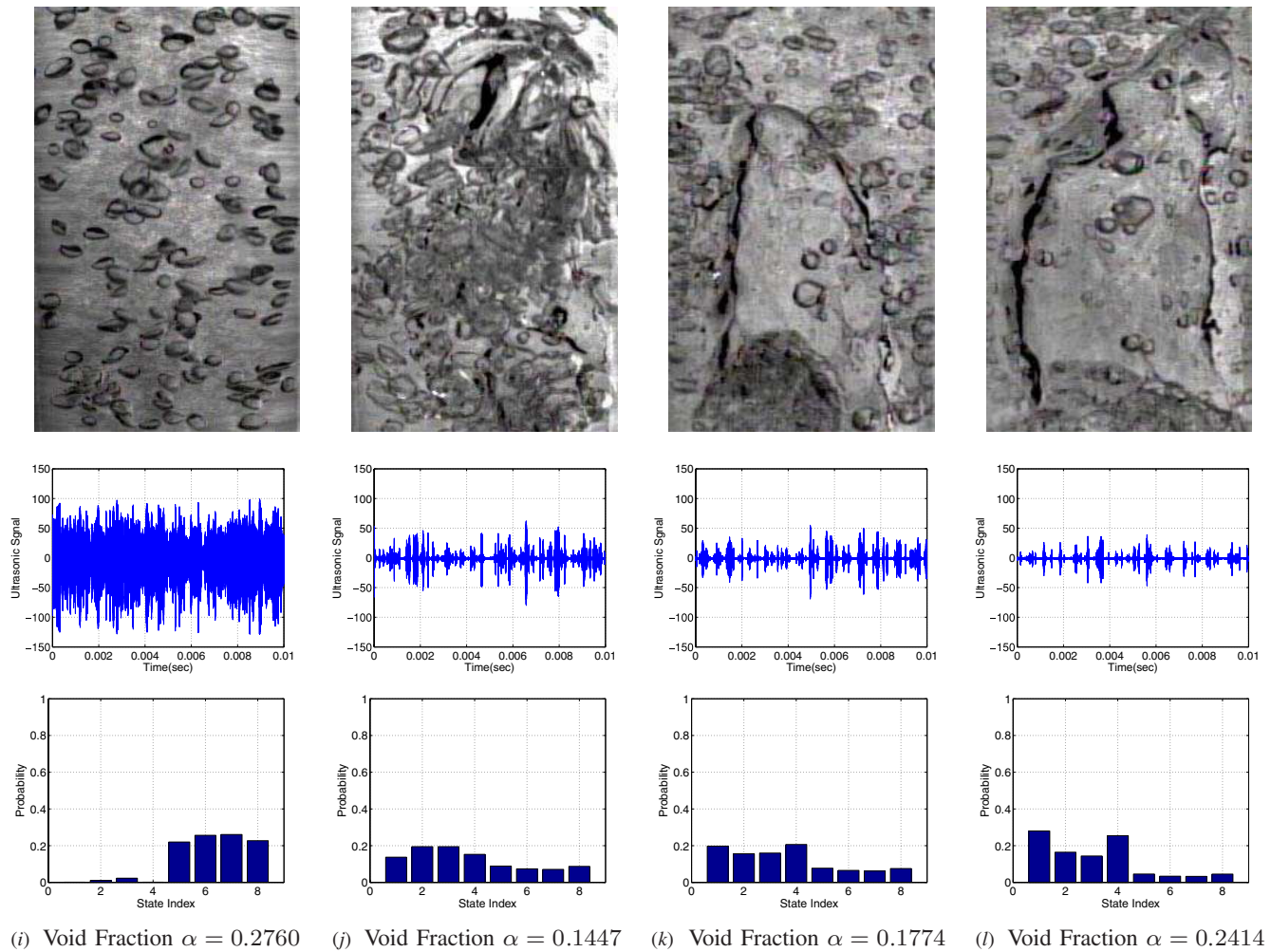


**Figure 2.** Rows from top to bottom: (1) high-speed camera image of the flow process; (2) ultrasonic signal; (3) pattern (i.e., state probability) vector.

**Table 1.** Table showing estimated superficial gas velocity and void fraction.

Run number	1	2	3	4	5	6	7	8	9	10	11
Superficial gas velocity ( $\text{cm s}^{-1}$ )	0	0.41	0.83	1.24	2.07	2.90	4.20	5.46	6.81	8.52	10.22
Void fraction	0	2.76	4.90	7.87	12.26	14.47	16.61	17.74	20.23	22.73	24.14

The flow rate is manually incremented from the nominal quiescent zero-air-flow condition to the full-flow condition of  $\sim 200 \text{ cm}^3 \text{ s}^{-1}$  in ten steps. At each flow condition ultrasonic data from the Panametrics ultrasonic transducer are recorded, and at the same time, the readings from the conductivity probe are measured at nine individual spatial locations along the radial direction. Table 1 shows the superficial gas velocity in  $\text{cm s}^{-1}$  and the estimated void fraction data for each flow condition.

#### 4. Results and discussion

Figure 2 exhibits the evolution of the two-phase air–water flow process and the results of analysis at four different epochs. The top row in figure 2 shows four images of the flow field captured by a high speed camera at different void fractions. Time-

series of the ultrasonic data at the same four flow conditions are displayed in the middle row. For ASSP of the time series data described in section 2, maximum entropy partitioning is employed in the radial direction with  $|\Sigma_R| = 2$ , while using uniform partitioning in the angular direction with  $|\Sigma_A| = 4$ . Thus, the alphabet size  $|\Sigma| \triangleq |\Sigma_R| \times |\Sigma_A| = 8$  and a depth of  $D = 1$  have been selected. The selection of  $|\Sigma|$  and  $D$  is made as a trade-off between capability of void-fraction detection and robustness to measurement noise. The pattern vector obtained by constructing the  $D$ -Markov machine is a representation of the dynamical system that characterizes the two-phase flow process in general. The state probability vectors are shown as histograms at the bottom row in figure 2. This visualization displays how the structure of the underlying probability distribution changes as the (spatially averaged) void fraction  $\alpha$  evolves in the two-phase flow process.

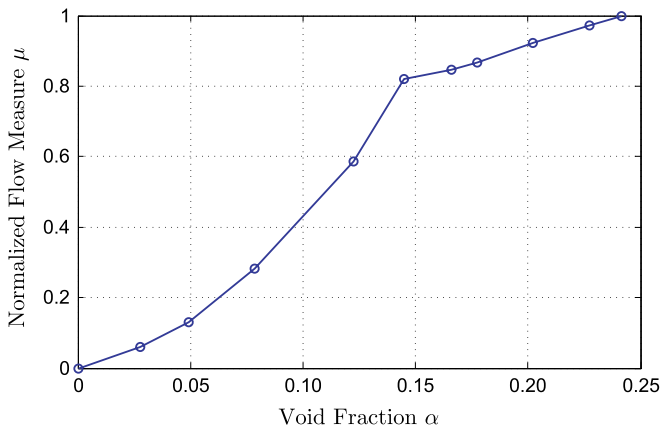


**Figure 3.** Profile of the flow measure  $\mu$  under evolving void fraction  $\alpha$ .

The angle measure in equation (5) has been used to quantify the departure of the flow pattern from its nominal operating condition, selected as no air flow (i.e.,  $\alpha = 0$ ), for the present analysis. The information on gradual evolution of the flow characteristics is assimilated in the form of a profile of normalized flow measure  $\mu$  versus the (spatially averaged) void fraction  $\alpha$ , as seen in figure 3. The most notable feature of the plot in figure 3 is its smooth monotonicity that ensures a one-to-one mapping of the flow condition to the flow measure  $\mu$ . It is also noted that the flow measure plot shows a well-defined change in the slope and curvature at a void fraction  $\alpha \approx 0.1447$ , which signifies a transition from one flow regime to another. Apparently, the images from the high speed camera show a transition from fully bubbly flow to cap-bubbly flow in the vicinity of  $\alpha \approx 0.1447$ .

## 5. Summary, conclusions and future work

This communication presents an application of the recently reported theories of symbolic dynamic filtering SDF [14] and analytic signal space partitioning (ASSP) [15] for void fraction measurement and identification of two-phase flow regimes. The experimental results, obtained on a laboratory-scale test apparatus, suggest that there exists a one-to-one correspondence between the flow measure derived from symbolic dynamic filtering and the void fraction measured by spatial averaging of local measurements of a conductivity probe. A sharp change in the slope of flow measure has been found to be in agreement with a transition from fully bubbly flow to cap-bubbly flow. Based on the analysis of these experimental results, it is reasonable to conclude that the proposed measurement technique has the potential of emerging into a useful non-intrusive tool for measurement of void fraction and identification of flow regimes in two-phase flow processes. However, further theoretical, computational and experimental research is necessary before the proposed two-phase flow monitoring technique can be considered for industrial applications (e.g., nuclear power reactor plants, petroleum industry and micro-gravity flow systems). Specifically, the following issues have been

identified, which are of significant interest in field applications and demand future research initiatives.

One of the major areas of interest is to establish versatility of the proposed technique in different applications. The flow characteristics are dependent on but are not limited to void fractions in the flow process, the pipe diameter and geometry, the temperature of the fluid and the fluid velocity. The geometry and material of the pipe also affect the strength of ultrasonic signals and their characteristics. The proposed method of void fraction measurement and detection of flow regime changes is a step towards building a robust, and material and geometry independent flow recognition method by taking advantage of non-intrusive single sensor measurements. It is noted that this independence is implicitly built into the algorithm, since the pattern (i.e., the state probability vector) at any flow condition through a pipe of a certain geometry and material is compared with the nominal signal for the same pipe, rather than being an absolute measurement. This property of the proposed method makes the observed deviations isolated from these extraneous factors, and hence are more directly related to the change in the flow characteristics alone. However, this postulation needs to be justified by experimental evidence. Validation of this deviation-monitoring algorithm, and investigation on its possible insensitivity to pipe geometry and pipe wall material have been planned. In addition, the reflections directly from the liquid/gas interface, measured by single or multiple ultrasonic transducers, are a potential source of information, in particular, at high void fractions.

To investigate the above research issues, a more advanced test apparatus, consisting of different channel geometries and flow orientations, is being developed.

## References

- [1] Chien K H, Chen T T, Pei B S and Lin W K 1997 Void fraction measurement by using the side-tube method *Flow Meas. Instrum.* **8** 103–12
- [2] Okawa T, Kubota H and Ishida T 2007 Simultaneous measurement of void fraction and fundamental bubble parameters in subcooled flow boiling *Nucl. Eng. Des.* **237** 1016–24
- [3] Mishima K, Hibiki T and Nishihara H 1997 Visualization and measurement of two-phase flow by using neutron radiography *Nucl. Eng. Des.* **175** 25–35
- [4] Mishima K and Hibiki T 1998 Development of high-frame-rate neutron radiography and quantitative measurement method for multiphase flow research *Nucl. Eng. Des.* **184** 183–201
- [5] Mi Y 1998 Two-phase flow characterization based on advanced instrumentation, neural networks, and mathematical modeling *PhD Thesis* Purdue University
- [6] Yang H C, Kim D K and Kim M H 2003 Void fraction measurement using impedance method *Flow Meas. Instrum.* **14** 151–60
- [7] Neal L G and Bankoff S G 1963 A high resolution resistivity probe for determination of local void properties in gas-liquid flow *AIChE J.* **9** 490–4
- [8] Kim S, Fu X Y, Wang X and Ishii M 2000 Development of the miniaturized four-sensor conductivity probe and the signal processing scheme *Int. J. Heat Mass Transfer* **43** 4101–18
- [9] Xu L J and Xu L A 1997 Gas/liquid two-phase flow regime identification by ultrasonic tomography *Flow Meas. Instrum.* **8** 145–55

- [10] Supardan M D, Masuda Y and Uchida S M 2007 The investigation of gas holdup distribution in a two-phase bubble column using ultrasonic computer tomography *Chem. Eng. J.* **130** 125–33
- [11] Bieberle M, Schleicher E and Hampel U 2008 Simulation study on electron beam x-ray ct arrangements for two-phase flow measurements *Meas. Sci. Technol.* **19** 094003
- [12] Schleicher E, Silva M J da, Thiele S, Li A, Wollrab E and Hampel U 2008 Design of an optical tomograph for the investigation of single- and two-phase pipe flows *Meas. Sci. Technol.* **19** 094006
- [13] Zhou W, Suzuki T, Nishiumi T and Yamamoto F 2008 Reconstruction of gas-liquid flows using the stochastic estimation with 16-channel electrode array *Meas. Sci. Technol.* **19** 105402
- [14] Ray A 2004 Symbolic dynamic analysis of complex systems for anomaly detection *Signal Process.* **84** 1115–30
- [15] Subbu A and Ray A 2008 Space partitioning via Hilbert transform for symbolic time series analysis *Appl. Phys. Lett.* **92** 084107
- [16] Cohen L 1995 *Time-Frequency Analysis* (Upper Saddle River, NJ: Prentice Hall PTR)
- [17] Lee J Y, Kima N S and Ishii M 2008 Flow regime identification using chaotic characteristics of two-phase flow *Nucl. Eng. Des.* **238** 945–57
- [18] Ott E 2003 *Chaos in Dynamical Systems* 2nd edn (Cambridge: Cambridge University Press)